

# Mechanism of oxidative stress and Keap-1/Nrf2 signaling pathway in bronchopulmonary dysplasia

Di Ma, MD, Wenhui Gao, MD, Junjiao Liu, MD, Dan Kong, MD, Yunfeng Zhang, MD, Min Qian, MD, PhD\*

## Abstract

Bronchopulmonary dysplasia (BPD) is a chronic lung disease common in premature infants and is one of the leading causes of disability and death in newborns. The Keap-1/Nrf2 signaling pathway plays an important role in antioxidant and anti-inflammatory.

Ten clean-grade, healthy pregnant Sprague-Dawley rats (purchased from Experimental Animal Center of Peking university, China) naturally gave birth to 55 neonatal rats from which 40 were selected and randomly divided into a hyperoxia group and a control group (N=20, each). Thirty-two BPD patient samples are from Neonatal Department of the second Hospital of Jilin University from November 30, 2016 to May 1, 2019.

In present study, we observed that lung tissues of the control group did not undergo obvious pathological changes, whereas in the hyperoxia group, lung tissues had disordered structures. With increased time of hyperoxia exposure, the alveolar wall became attenuated. Under hypoxia conditions, the activity of oxidative stress-related enzymes (CAT, GSH-Px, SOD) in lung samples was significantly lower than that before treatment. The expression level of Keap1 mRNA and protein in the hyperoxia group was slightly lower than that of control group. The expression of Nrf2 and HO-1 mRNA and protein in the hyperoxia group was significantly higher than that of control group. For the infants with BPD, we found that the activity of SOD, GSH-Px, and CAT was significantly different from those of control group.

We constructed a premature BPD animal model and found the abnormal of oxidative stress in different groups and the expression levels of Keap1/Nrf2 signaling pathway-related molecules, and we validated the results in premature infants with BPD.

**Abbreviations:** BPD = bronchopulmonary dysplasia, Keap1 = Kelch-like ECH-associated protein 1, Nrf2 = transcription factor NF-E2 p45-related factor 2.

**Keywords:** BPD, Keap-1/Nrf2, oxidative stress

## 1. Introduction

Bronchopulmonary dysplasia (BPD) is the most common chronic lung disease of premature infants and is caused by mechanical ventilation and oxygen therapy after acute respiratory distress. In some extreme cases, it may lead to severe complications. The mortality rate of BPD is >30% because of chronic lung dysfunction and lung dysplasia.<sup>[1-4]</sup> BPD is caused by a variety of factors, which can be divided into individual factors (such as

premature birth, sex, genetic susceptibility, and so on), iatrogenic factors (such as hyperoxia, mechanical ventilation, blood transfusion, and so on), and external factors (prenatal infection, postpartum infection, and so on). At present, the basic research on BPD focuses on the development of capillary blood vessels in the lungs. It is found that pulmonary capillary development is an important part of alveolar septal formation during BPD alveolarization.<sup>[5-7]</sup> During development, the double capillary layer fuses into a single layer of endothelium and gradually binds to the adjacent alveolar epithelial basement membrane to form an adult-like blood-sparing barrier. At the same time as interstitial thinning and vascularization occur, the air column columnar epithelial cells differentiate into squamous epithelial cells, which prolongs the airway, thickens the tube diameter, and enhances gas exchange capacity.<sup>[8]</sup> Studies have found that if the formation of capillary blood vessels in the lungs of newborn mice is inhibited, the alveolar structure of mice is simplified, and the histopathological features are consistent with those of children with BPD. Vascular endothelial growth factor is an important cytokine that promotes angiogenesis and plays an important role in angiogenesis. It is argued that some biomarkers increase the susceptibility to BPD. Some cellular or humoral biomarkers contribute to the pathogenesis of BPD. These biomarkers can be both mediators of pathophysiology and biomarkers of the disease.<sup>[9]</sup>

It is generally believed that BPD is based on genetic susceptibility, and various adverse factors such as oxygen poisoning, barotrauma or volume injury, and infection cause damage to immature lungs and abnormal repair of lung tissue

Editor: Uddyalok Banerjee.

The authors report no conflicts of interest.

The datasets generated during and/or analyzed during the current study are available from the corresponding author on reasonable request.

The second Hospital of Jilin University, Neonatal Department, Changchun, Jilin, China.

\* Correspondence: Min Qian, Professor and Chief director., No. 218 Ziqiang street, Changchun, Jilin Province 130000, PR China (e-mail: chentaosyu@126.com).

Copyright © 2020 the Author(s). Published by Wolters Kluwer Health, Inc. This is an open access article distributed under the terms of the Creative Commons Attribution-Non Commercial License 4.0 (CCBY-NC), where it is permissible to download, share, remix, transform, and buildup the work provided it is properly cited. The work cannot be used commercially without permission from the journal.

How to cite this article: Ma D, Gao W, Liu J, Kong D, Zhang Y, Qian M. Mechanism of oxidative stress and Keap-1/Nrf2 signaling pathway in bronchopulmonary dysplasia. *Medicine* 2020;99:26(e20433).

Received: 7 October 2019 / Received in final form: 17 March 2020 / Accepted: 27 April 2020

<http://dx.doi.org/10.1097/MD.00000000000020433>

after injury. High concentration of oxygen can cause nonspecific changes such as pulmonary edema, inflammation, fibrin deposition, and decreased activity of pulmonary surfactant, and form highly active oxygen-free radicals in the body. Oxygen-free radicals are the key inflammatory mediators in the pathogenesis of BPD.<sup>[10–12]</sup> Oxidative stress plays an important role in the pathogenesis of BPD.<sup>[13]</sup>

Transcription factor NF-E2 p45-related factor 2 (Nrf2, gene name *NFE2L2*) regulates the expression of a large network of genes encoding inducible cytoprotective proteins that allow mammalian cells and organisms to adapt and survive under various conditions including oxidative stress. Together with its principal negative regulator, Kelch-like ECH-associated protein 1 (Keap1), Nrf2 forms a molecular effector and sensor system that robustly responds to perturbations of the cellular redox balance and orchestrates a comprehensive defense program, which in turn restores homeostasis.<sup>[14,15]</sup> The Nrf2 status affects the production of ROS by the 2 major ROS producing systems, mitochondria and NADPH oxidase. Among the Nrf2 transcriptional targets are proteins with critical roles in the generation and utilization of reducing equivalents such as NADPH and reduced glutathione (GSH), as well as thioredoxin, thioredoxin reductase, peroxiredoxin, and sulfiredoxin, which collectively provide compartmentalized redox sensing of ROS to maintain redox balance under homeostatic conditions.<sup>[16,17]</sup>

This study aimed to explore the Keap1/Nrf2 signaling pathway affecting the oxidative-antioxidant balance through regulation of oxidative stress, thereby regulating the pathogenesis of bronchopulmonary dysplasia. In this study, we constructed a premature BPD animal model to detect the levels of oxidative stress in different groups and the expression levels of Keap1/Nrf2 signaling pathway-related molecules, and to clarify the important role of Keap1/Nrf2 signaling pathway in bronchopulmonary dysplasia in premature infants.

## 2. Patients and methods

### 2.1. Experimental animals and modeling

Ten clean-grade, healthy pregnant Sprague-Dawley rats (purchased from Experimental Animal Center of Peking university, China) naturally gave birth to 55 neonatal rats from which 40 were selected (2–3 days' old, either sex) and randomly divided into a hyperoxia group and a control group (N=20, each). All rats were free fed for 12 continuous weeks. An oxygen tank was made by our group, on which an air inflow hole, an air outflow hole, and an oxygen-measuring hole were set. The air inflow hole was connected to oxygen and the oxygen-measuring hole was connected with a CY-100 digital oxygen measurement device. Solid barium hydroxide was put in the oxygen tank to adsorb carbon dioxide, with the temperature maintained at 22° to 26°C and the humidity kept at 65% to 75%. For the hyperoxia group, 20 neonatal rats and 2 female rats were placed inside the oxygen tank, where oxygen flow was controlled at 6L/min and the concentration was maintained  $\geq 95\%$  and continuously monitored. For the control group, 20 neonatal rats and 2 female rats were put inside a standard rat cage and continuously fed in the same room. Drinking water and food were added at a fixed time every day. Additionally, bedding and solid barium hydroxide were refreshed when needed. The growth, development, respiration, and activities of the rats were recorded. To prevent the female rats from oxygen poisoning-induced decreases in

feeding and nursing abilities, they were switched on a regular basis. On the 1st, 3rd, and 7th days, 8 neonatal rats were randomly selected from each group and sacrificed after anesthesia through intraperitoneal injection of 10% chloral hydrate (8–10 mg/kg), after which lung tissues were sampled.

### 2.2. Sampling and treatment

The neonatal rats were sacrificed after anesthesia. After the thoracic cavity was scissored open, bilateral lungs were rapidly taken out and rinsed repeatedly with normal saline. Then, tissues of the right lung were put in an Eppendorf tube, frozen with liquid nitrogen, and stored at  $-80^{\circ}\text{C}$  before real-time quantitative polymerase chain reaction (PCR) and western blotting. Tissues of the left lung were fixed in 4% paraformaldehyde for 24 hours, washed with water, dehydrated with serial concentrations of ethanol, made transparent with dimethylbenzene, paraffin-embedded, and prepared into 5-mm thick sections.

### 2.3. Patient selection and study design

Our study was a case-control study conducted in the Neonatal Department of the second Hospital of Jilin University from November 30, 2016 to May 1, 2019. All applicable international, national, and/or institutional guidelines for the care and use of animals were followed. All procedures performed in studies involving human participants were in accordance with the ethical standards of the institutional and/or national research committee and with the 1964 Helsinki declaration and its later amendments or comparable ethical standards. The study was approved by the Regional Ethical Review Board for the second Hospital of Jilin University. The approval number was SJL455832. All parents signed the informed consent before the study. All infants with gestational age (GA) of  $<32$  weeks and birth weight (BW) of  $<1500$  g were followed in NICU. Infants with moderate or severe BPD were included in the study group. BPD was defined according to oxygen requirement or positive pressure ventilation therapy for a certain period (days) (eg, at postmenstrual age [PMA] 36 weeks or over postnatal day 28). Mild BPD was considered for infants who had oxygen requirement throughout the first 28 days but not at 36 weeks of PMA or at discharge. Moderate BPD was identified as oxygen requirements over 28 days of postnatal life plus oxygen supplementation with  $<30\%$  oxygen level at 36 weeks of PMA. Severe BPD was defined as oxygen dependence with  $\geq 30\%$  oxygen requirement over the first 28 days of postnatal life and/or positive pressure support at 36 weeks of PMA.

### 2.4. Blood sampling

Umbilical cord blood samples were obtained from infants with GA  $<32$  weeks and BW  $<1500$  g. Subsequently, blood samples were obtained from infants who were diagnosed with moderate or severe BPD at 36 weeks of PMA. Also, blood samples for the measurement of IL-33 were obtained before starting and after HC treatment. The levels of IL-33 were evaluated in the control group at 36th week of PMA. Simple glass tubes covering no separation gel or preservatives were used for the collection of blood samples. Clotting of blood was waited for a while (30 minutes) at  $4^{\circ}\text{C}$ , and subsequently centrifuged at 3000 rpm at  $4^{\circ}\text{C}$  for 10 minutes. One milliliter of serum aliquots were separated and frozen at  $-80^{\circ}\text{C}$  until evaluation. Before starting measure-

ment, serum samples with a trace amount of hemolysis were rejected and completely excluded from the study.

### 2.5. Antioxidant status in blood samples and rats tissues

Catalase (CAT), glutathione peroxidase (GSH-Px), and superoxide dismutases (SOD) were measured in tissue homogenates. Samples were run in duplicates, and the manufacturer's instructions were followed for conducting this assay after reconstituting tissue lysates and diluting them in the MAPAssay Buffer. The plates were analyzed using the Luminexw system. Data were normalized to total protein concentration before analysis and reported as median fluorescence intensity.

### 2.6. RNA extraction and real-time reverse transcriptase-PCR

Total RNA of tissue samples were isolated using TRIzol (Life Technologies, Inc., Rockville, MD) according to the manufacturer's instructions. cDNA was generated from 1  $\mu$ g of each RNA sample and a reverse transcribed using a transcription kit (Takara, Kyoto, Japan). Real-time quantitative reverse transcriptase-PCR (qRT-PCR) was done in the 7300 Real Time PCR System (Applied Biosystems).

### 2.7. Western blotting analysis

Denatured protein samples were resolved on SDS-PAGE and transferred to PVDF membrane (Millipore, Billerica, MA). After blocking with non-fat milk, membrane was incubated overnight at 4°C with antibodies including Keap-1, Nrf2, HO-1, and  $\beta$ -actin (Abcam) followed by incubation with the antirabbit HRP-conjugated secondary antibodies (Santa Cruz, Billerica, MA). Chemiluminescence detection was performed using ECL advance Western blotting detection reagents (GE healthcare, Little Chalfont, Buckinghamshire, UK). The relative expression was quantified by image software (Fig. 1).

### 2.8. Statistical methods

Continuous variables were expressed as mean  $\pm$  SD (standard deviation) and compared using a 2-tailed unpaired Student *t* test;

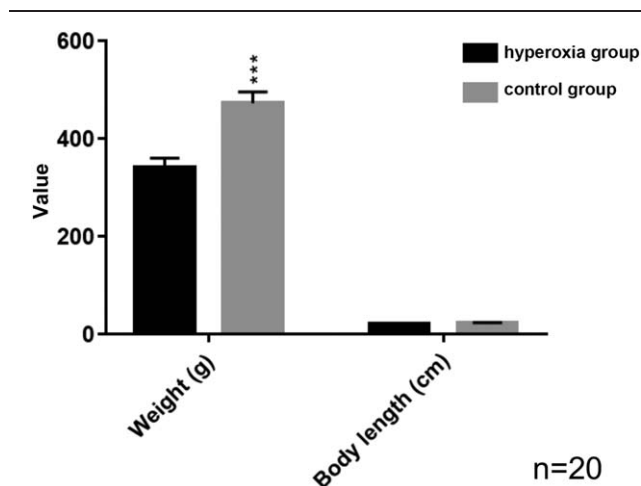


**Figure 1.** Comparison the body weight and body length in different groups ( $P < .01$ ).

categorical variables were compared using  $\chi^2$  or Fisher analysis. All statistical evaluations were carried out using SPSS software (Statistical Package for the Social Science, version 15.0, SPSS Inc, Chicago, IL). A value of  $P < .05$  was considered to be statistically significant in all the analyses.

## 3. Results

### 3.1. General state of animals

The control group rats grew normally and the hyperoxia group gradually became emaciated and sluggish, with the body weight and body length rising slowly. The body weight and body length increased by 2 to 3 g/day and 1.0 to 1.5 cm/day in the control group, whereas body weight and body length did not increase in the hyperoxia group, respectively. Three rats in the hyperoxia group died on the 5th and 6th days. The total mortality rate was 15%. The dead rats were discarded and lung tissues were not sampled.

### 3.2. Morphological changes of lung tissues

Under a low-power microscope (100X magnification), lung tissues of the control group did not undergo obvious pathological changes. The alveoli were clearly structured and uniformly sized. The alveolar space was small, without liquid or inflammatory exudate, and the alveolar septum was thick (Fig. 2A and B). In the hyperoxia group, lung tissues had disordered structures. With increased time of hyperoxia exposure, the alveolar wall became attenuated, and the alveoli decreased and became structurally simplified and nonuniformly sized. Some alveoli fused and became enlarged. The alveolar area was reduced and the diameter of alveolar space evidently increased. There was exudation of a small number of inflammatory cells inside the alveolar space and a thin alveolar septum. Since interstitial lung fibroblasts and collagen-like substance increased locally, differentiation and development of the lung were blocked. Under a high-power microscope (400 $\times$  magnification), the control group had integral alveolar walls and there was no evidence of exfoliated cells inside the alveoli. In contrast, alveoli of the hyperoxia group had erythrocytes, macrophage exudate, and exfoliated lung epithelial cells. Additionally, the alveolar septum was thickened, interstitial cells increased, and small blood vessels dilated and became congested (Fig. 2C and D).

### 3.3. Detection, comparison of CAT, GSH-Px, and SOD activities in lung samples in different groups

Under hypoxia conditions, the activity of oxidative stress-related enzymes (CAT, GSH-Px, SOD) in lung samples was significantly lower than that before treatment ( $P < .05$ ). The details were shown in Figure 3.

### 3.4. Detection and comparison of mRNA expression levels and protein levels of antioxidation-related genes Keap1, Nrf2, and HO-1 in lung samples in different groups

The mRNA expression levels of Keap1, Nrf2, and HO-1 in the lung tissues of the 2 groups were detected by qRT-PCR. The results showed that the expression level of Keap1 mRNA in the hyperoxia group was slightly lower than that of control group ( $P < .05$ , Fig. 4A and B). The expression of Nrf2 mRNA in the

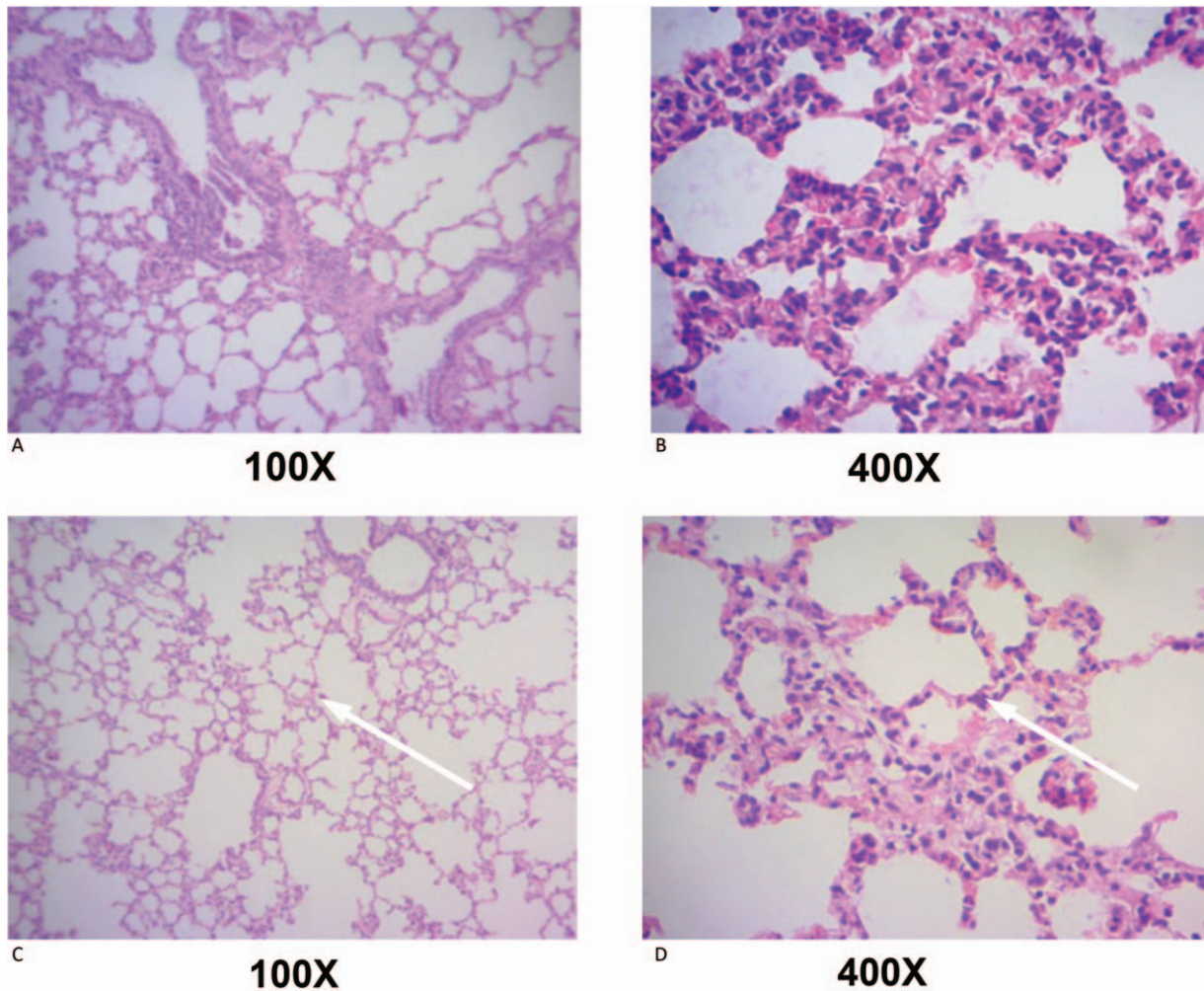


**Figure 2.** Morphological changes in lung tissues under the low-power microscope (H&E; 100×) and the high-power microscope (H&E; 400×).

hyperoxia group was significantly higher than that of control group ( $P < .001$ , Fig. 4C and D). HO-1 mRNA expression in the hyperoxia group was significantly higher than that of control group ( $P < .001$ , Fig. 3E and F). The protein expression levels of *Keap1*, *Nrf2*, and *HO-1* in the lung tissues of the 2 groups were detected by western blot. The similar trend of these 3 factors was observed in Figure 5A and B.

**3.5. Comparison of clinical characteristics and oxidative stress-related enzymes between control group and BPD group**

There were no significant differences in maternal age, sex, and delivery mode between the 2 groups of patients ( $P > .05$ ). There were significant differences in the gestational age, time of hospital

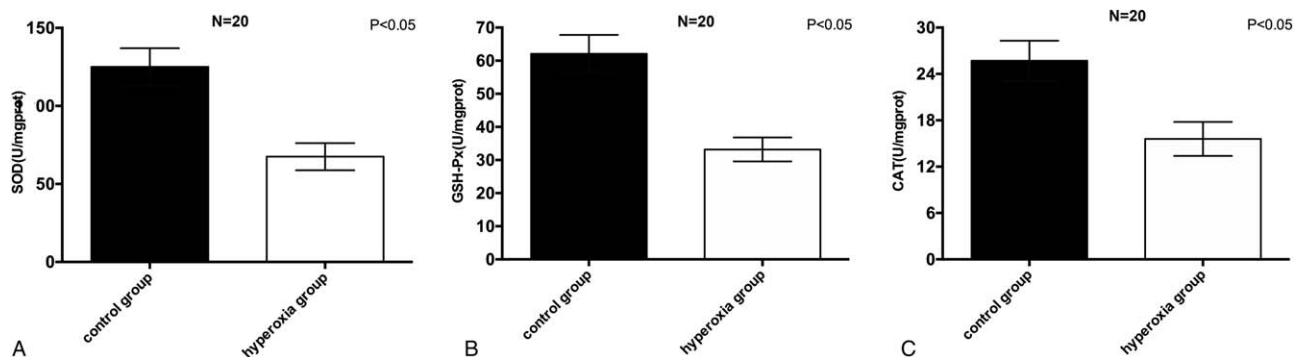


**Figure 3.** the activity of oxidative stress-related enzymes (CAT, GSH-Px, SOD) in lung samples was significantly lower than that before treatment ( $P < .05$ ).

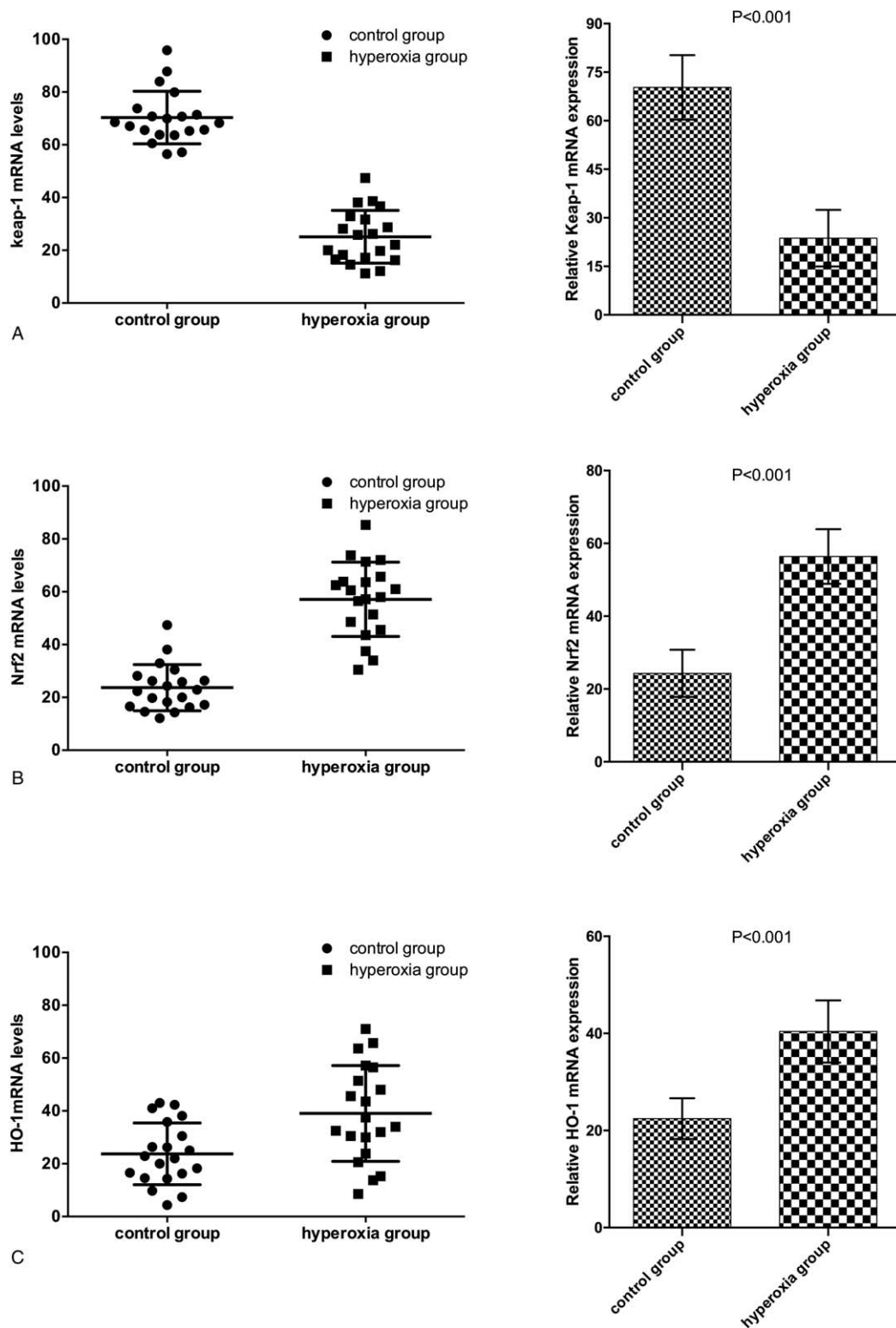


**Figure 4.** Detection and comparison of mRNA expression levels of anti-oxidation related genes Keap1, Nrf2, and HO-1 in lung samples in different groups.

staying, and Apgar score first minute between the control group and BPD group (Table 1). The activities of oxidative stress-related active enzymes in patients with BPD were further confirmed by detecting and comparing the activities of CAT, GSH-Px, and

SOD in blood samples. The results showed that the activity of SOD ( $P < .01$ ), GSH-Px ( $P < .01$ ), and CAT ( $P < .01$ ) in BPD group were significant different from those of control group (Table 1).

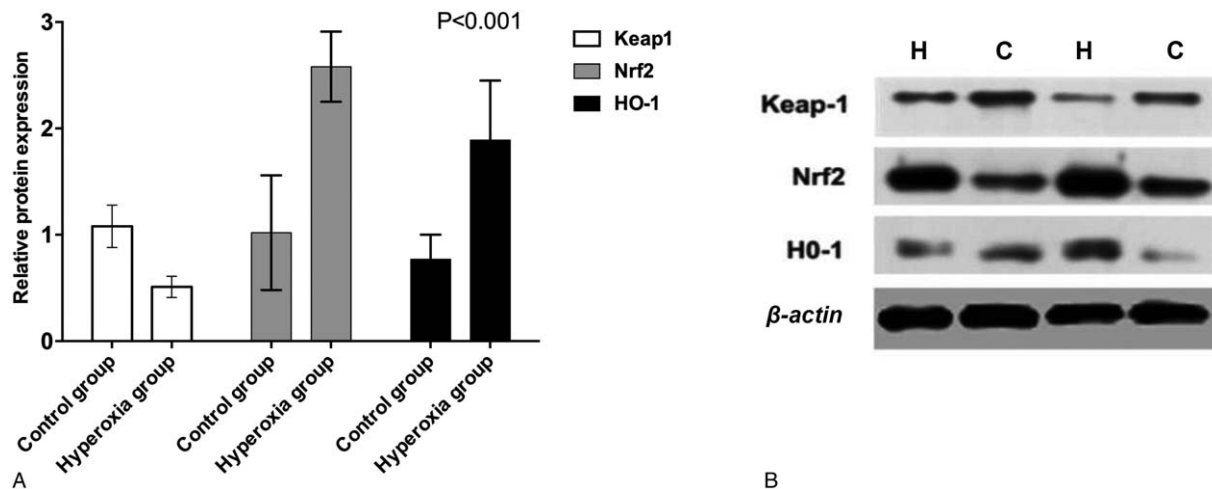


**Figure 5.** Detection and comparison of protein levels of antioxidant-related genes Keap1, Nrf2, and HO-1 in lung samples in different groups.

#### 4. Discussion

BPD, first described in 1967 by Northway et al, was defined as pulmonary disease due to mechanical ventilation in premature infants with respiratory distress syndrome.<sup>[18]</sup> Subsequently, the National Institute of Health consensus conference defined BPD as mild, moderate, or severe according to respiratory support at 28 days of age and 36 weeks of PMA.<sup>[7]</sup> The survival rate of preterms increases due to significant advances in respiratory care in the newborn. However, BPD is still an important clinical problem as the most common pulmonary morbidity. In addition to the genetic predisposition,

During the first stage of an oxidative stress, Nrf2 is activated via the disassociation of Nrf2 from its repressor protein in the cytoplasm, Keap-1, which contains cysteine residues. In detail, Keap-1 reacts with oxidative and electrophilic radicals leading to conformational changes and the release of Nrf2.<sup>[19,20]</sup> Subsequently, the translocation of Nrf2 to the nucleus takes place and it binds to antioxidant response element resulting in the transcription of defensive genes.<sup>[21]</sup> The activation of the transcription involves Nrf2 recognizing its own promoter and establishing an effective interaction with it and the newly formed and

accumulated Nrf2 in the nucleus binds to promoters of other specific genes.<sup>[22]</sup>

In present study, we observed that lung tissues of the control group did not undergo obvious pathological changes whereas in the hyperoxia group, lung tissues had disordered structures. With increased time of hyperoxia exposure, the alveolar wall became attenuated. Under hypoxia conditions, the activity of oxidative stress-related enzymes (CAT, GSH-Px, SOD) in lung samples was significantly lower than that before treatment. The expression level of Keap1 mRNA and protein in the hyperoxia group was slightly lower than that of control group. The expression of Nrf2 and HO-1 mRNA and protein in the hyperoxia group was significantly higher than that of control group. For the infants with BPD, we found that the activity of SOD, GSH-Px, and CAT was significantly different from those of control group.

The present study has several limitations. There are some previously reported prognostic factors which were not included in this study, such as the comorbidities accompanied with BPD and the management of antenatal steroid. Moreover, the clinical work in this study was insufficient and more further studies are needed in the future. In this study, the clinical results were primary and further studies are need to demonstrate the potential mechanism of Keap1/Nrf2 signaling pathway in BPD.

In conclusion, we constructed a premature BPD animal model and found the abnormal of oxidative stress in different groups and the expression levels of Keap1/Nrf2 signaling pathway-related molecules, and we validated the results in Wpremature infants with BPD.

#### Author contributions

**Conceptualization:** Di Ma, Min Qian.

**Data curation:** Min Qian.

**Formal analysis:** Di Ma.

**Investigation:** Junjiao Liu, Dan Kong.

**Methodology:** Wenhui Gao, Junjiao Liu, Dan Kong.

**Project administration:** Wenhui Gao.

**Resources:** Wenhui Gao, Dan Kong.

**Software:** Di Ma, Dan Kong.

**Supervision:** Di Ma.

**Table 1**

**Demographics and clinical characteristics of all patients.**

Variables	Control group	BPD group	P
Case (n)	32	32	
Maternal age, y	30.2±3.8	29.3±4.6	>.05
Gestational age (wks, days)	29.6±1.6	26.3±3.1	<.05
Sex: male/female	18/14	15/17	>.05
Hospital stay, days	35.3±16.7	56.2±12.4	<.01
Mode of delivery, n (%)			
Vaginal delivery	12	10	>.05
Apgar score first minute	8 (4–9)	6 (3–7)	<.05
SOD levels	158.6±10.6	129.7±7.5	<.01
GSH-Px levels	120.7±9.2	79.3±8.2	<.01
CAT levels	3500.2±2.8	2601.7±8.5	<.01

BPD = bronchopulmonary dysplasia, CAT = catalase, GSH-Px = glutathione peroxidase, SOD = superoxide dismutases.

**Validation:** Min Qian.

**Visualization:** Min Qian.

**Writing – original draft:** Di Ma, Min Qian.

**Writing – review & editing:** Di Ma, Min Qian.

## References

- [1] Tracy MK, Berkelhamer SK. Bronchopulmonary dysplasia and pulmonary outcomes of prematurity. *Pediatr Ann* 2019;48:e148–53.
- [2] Principi N, Di Pietro GM, Esposito S. Bronchopulmonary dysplasia: clinical aspects and preventive and therapeutic strategies. *J Transl Med* 2018;16:36.
- [3] Hwang JS, Rehan VK. Recent advances in bronchopulmonary dysplasia: pathophysiology, prevention, and treatment. *Lung* 2018;196:129–38.
- [4] Bancalari E, Jain D. Bronchopulmonary dysplasia: can we agree on a definition? *Am J Perinatol* 2018;35:537–40.
- [5] Sung TJ. Bronchopulmonary dysplasia: how can we improve its outcomes? *Korean J Pediatr* 2019;62:367–73.
- [6] Singh JK, Wymore EM, Wagner BD, et al. Relationship between severe bronchopulmonary dysplasia and severe retinopathy of prematurity in premature newborns. *J AAPOS* 2019;23:209e1-209.e4.
- [7] Lecarpentier Y, Gourrier E, Gobert V, et al. Bronchopulmonary dysplasia: crosstalk between PPARgamma, WNT/beta-catenin and TGF-beta pathways; the potential therapeutic role of PPARgamma agonists. *Front Pediatr* 2019;7:176.
- [8] Hendricks-Munoz KD, Xu J, Voynow JA. Tracheal aspirate VEGF and sphingolipid metabolites in the preterm infant with later development of bronchopulmonary dysplasia. *Pediatr Pulmonol* 2018;53:1046–52.
- [9] Cakir U, Tayman C, Yucel C. A novel diagnostic marker for the severity of bronchopulmonary dysplasia in very low birth weight infants: interleukin-33. *Pediatr Allergy Immunol Pulmonol* 2019;32:12–7.
- [10] Torgerson DG, Ballard PL, Keller RL, et al. Ancestry and genetic associations with bronchopulmonary dysplasia in preterm infants. *Am J Physiol Lung Cell Mol Physiol* 2018;315:L858–69.
- [11] Reicherzer T, Haffner S, Shahzad T, et al. Activation of the NF-kappaB pathway alters the phenotype of MSCs in the tracheal aspirates of preterm infants with severe BPD. *Am J Physiol Lung Cell Mol Physiol* 2018;315:L87–101.
- [12] Balaji S, Dong X, Li H, et al. Sex-specific differences in primary neonatal murine lung fibroblasts exposed to hyperoxia in vitro: implications for bronchopulmonary dysplasia. *Physiol Genom* 2018;50:940–6.
- [13] Wang J, Dong W. Oxidative stress and bronchopulmonary dysplasia. *Gene* 2018;678:177–83.
- [14] Muller SG, Jardim NS, Quines CB, et al. Diphenyl diselenide regulates Nrf2/Keap-1 signaling pathway and counteracts hepatic oxidative stress induced by bisphenol A in male mice. *Environ Res* 2018;164:280–7.
- [15] Wang J, Jiang C, Zhang K, et al. Melatonin receptor activation provides cerebral protection after traumatic brain injury by mitigating oxidative stress and inflammation via the Nrf2 signaling pathway. *Free Radic Biol Med* 2019;131:345–55.
- [16] Ci X, Lv H, Wang L, et al. The antioxidative potential of farrerol occurs via the activation of Nrf2 mediated HO-1 signaling in RAW 264.7 cells. *Chem Biol Interact* 2015;239:192–9.
- [17] Zhu C, Dong Y, Liu H, et al. Hesperetin protects against H2O2-triggered oxidative damage via upregulation of the Keap1-Nrf2/HO-1 signal pathway in ARPE-19 cells. *Biomed Pharmacother* 2017;88:124–33.
- [18] Kicinski P, Malachowska B, Wyka K, et al. The level of extracellular superoxide dismutase in the first week of life in very and extremely low birth weight infants and the risk of developing bronchopulmonary dysplasia. *J Perinat Med* 2019;47:671–6.
- [19] Yu H, Zhang J, Ji Q, et al. Melatonin alleviates aluminium chloride-induced immunotoxicity by inhibiting oxidative stress and apoptosis associated with the activation of Nrf2 signaling pathway. *Ecotoxicol Environ Saf* 2019;173:131–41.
- [20] Zhang F, Munoz FM, Sun L, et al. Cell-specific regulation of Nrf2 during ROS-Dependent cell death caused by 2,3,5-tris (glutathion-S-yl)hydroquinone (TGHQ). *Chem Biol Interact* 2019;302:1–0.
- [21] Lu MC, Ji JA, Jiang ZY, et al. The Keap1-Nrf2-ARE pathway as a potential preventive and therapeutic target: an update. *Med Res Rev* 2016;36:924–63.
- [22] Fan J, Lv H, Li J, et al. Roles of Nrf2/HO-1 and HIF-1alpha/VEGF in lung tissue injury and repair following cerebral ischemia/reperfusion injury. *J Cell Physiol* 2019;234:7695–707.